2. Field scanning records

The pins in **Figure 2.1** show the locations of the structures that were scanned onsite. Owing to limited time, field-scanning areas close to the epicenters of the main shock and aftershocks were chosen. **Figure 2.1** shows the three areas in which a field survey was conducted. In the Antakya area, bridge sites were visited fewer times compared to in the Nurdağı and Malatya areas, because the main objective to visit the former was to explore other infrastructure facilities. The survey was conducted visually from the ground level for bridges and inside a moving vehicle for tunnels without a close-up view.

(Made using Google Maps)

Figure 2.1. Field-scanning areas and bridge locations scanned

2.1. Antakya city and Hatay Airport Road

2.1.1. Viaduct on D817 near Saraykent, Antakya city

(1) Date and location

The viaduct on D817 was scanned on March 10, 2023. **Figure 2.1-1** shows its location.

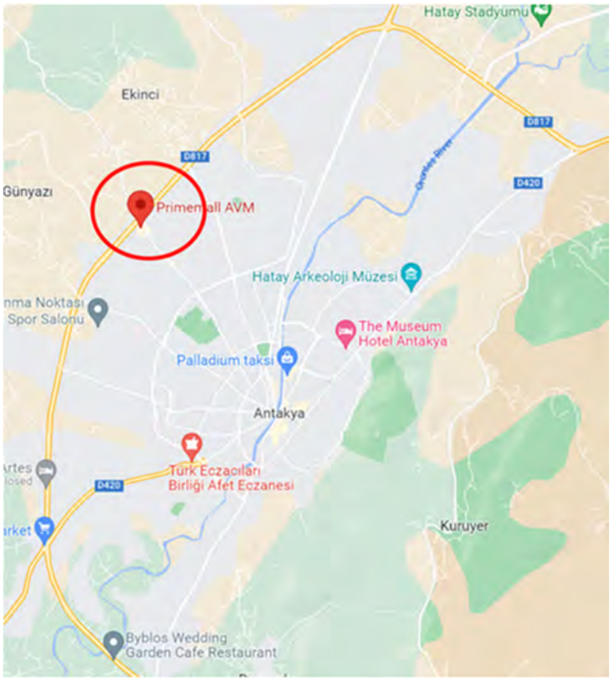

(Made using Google Maps)

Figure 2.1-1. Location of Viaduct on D817 near Saraykent, Antakya city

(2) General view

As shown in **Figure 2.1-2**, the bridge superstructure is divided for each direction and comprises of concrete I-girder beams with no end diaphragms. The floor slabs are continuous over intermediate piers.

Figure 2.1-2. Viaduct on D817 near Saraykent, Antakya city

(3) Findings

1) Southside abutment

As shown in **Figure 2.1-3**, the ends of the girders were damaged. Although the bridge did not collapse, its shear keys and girder ends were severely damaged. The concrete inside the vertical and horizontal reinforcing bars was damaged, and the reinforcing bars were deformed, indicating that the shear strength of the girder ends decreased significantly. Assuming that these girders are prestressed concrete beams, the present stress condition should be a significant concern because of the failure of the concrete cross-section. The spacing between the link slab support and the girder end was narrow, causing the girder ends to collide with the link slab support and the shear keys. There were no diaphragms at the girder ends. Theoretically, the energy generated by a collision could concentrate more on girder ends without an end diaphragm than on those with an end diaphragm. Another theory is that girder webs could be loaded transversely because of the inertial loads from the deck slab to the bearings or the shear keys and be damaged under out-of-plane flexure and shear in the absence of an end diaphragm.

Therefore, the seismic principles for controlling the location and form of damage in bridges must be studied. The damage to this bridge indicates that the lack of end transverse girders may severely exacerbate damage. Although seen from the inside of a moving vehicle, similar damage was observed on the girder ends on the abutment and the shear keys in another elevated bridge (same type) of D817 in the same city. Because several bridges have the same structural type and were similarly damaged, improving the typical structural details of their girder ends is recommended. Similar damage to concrete girder bridges was reported during the 2010 Chile Earthquake, and the effectiveness of a transverse diaphragm at girder ends has been discussed (Kawashima et al., 2011; Yen et al., 2011).

In addition, the existence of shear keys could hinder post-event inspection at the ground level. The spacing between the shear keys and the girders or between the link support and the girder ends of the bridge was extremely narrow to approach. Therefore, the effectiveness of designing a feasible process for inspecting girder ends and their surroundings should be studied.

Figure 2.1-3. Damage to girder ends and shear keys

2) Piers

On all piers, shear keys, link slabs, and girder ends were damaged (**Figure 2.1-4**), whereas no damage was found on the piers (**Figure 2.1-5**).

Figure 2.1-4. Examples of observed damage to girder ends and shear keys

Figure 2.1-5. Pier state at ground level and girder-end state above same pier

2.1.2. Bridges over Orontes River in downtown Antakya city

(1) Date and location

Bridges in downtown Antakya city were scanned on March 10, 2023. **Figure 2.1-6** shows the locations of the bridges scanned. Note that the bridges were not checked by hands-on close-view observations.

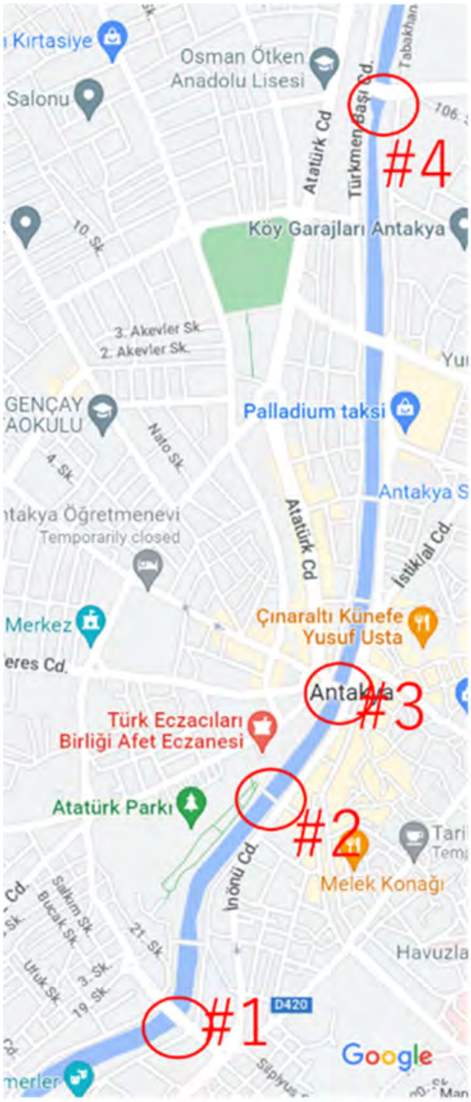

(Made using Google Maps)

Figure 2.1-6. Locations of bridges scanned in downtown Antakya city

(2) Bridge #1: Mehmet Yeloğlu Köprüsü (Figure 2.1-7)

Figure 2.1-7. Bridge #1

(3) Pedestrian bridges and roads around Bridge #1 (Figure 2.1-8)

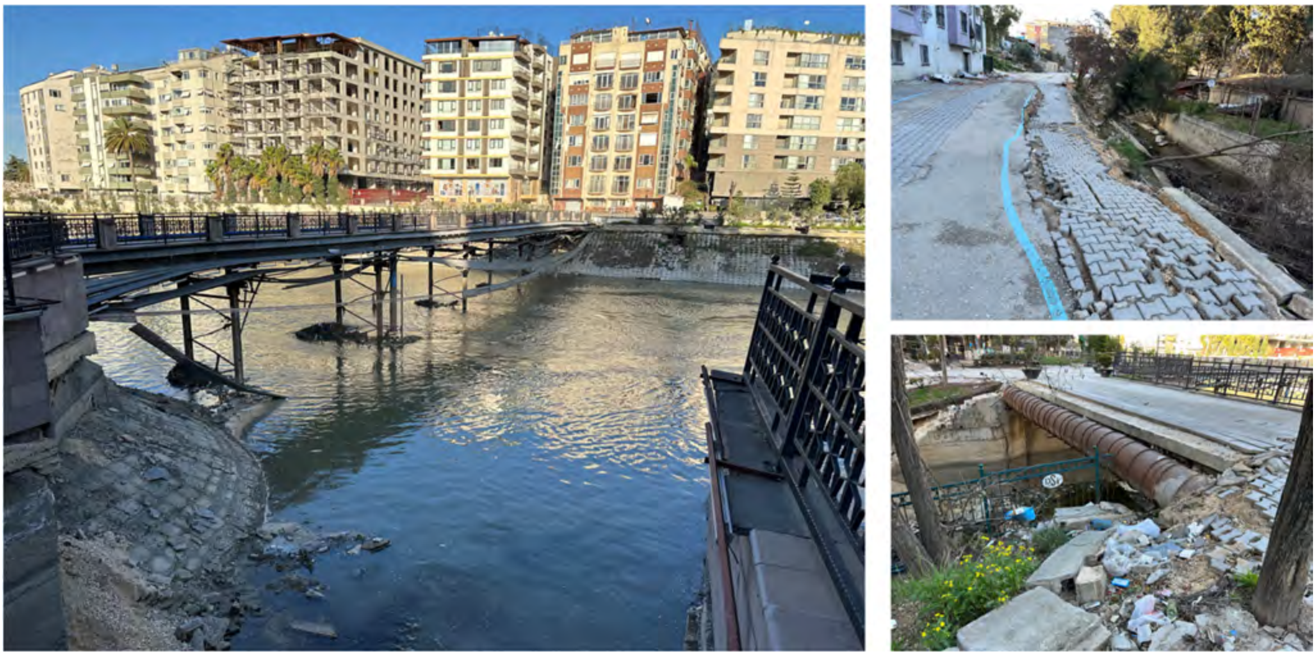

Figure 2.1-8. Pedestrian bridges and roads near Bridge #1

(4) Bridge #2 (Figure 2.1-9)

Figure 2.1-9. Bridge #2

(5) Bridge #3: Ata Köprüsü

Bridge #3 is a continuous steel girder with short spans. The conditions around the bearing were uncertain from the observation distance (**Figure 2.1-10**).

Figure 2.1-10. Bridge #3

There were cracks on the road surface behind the abutment (**Figure 2.1-11**). Surrounding buildings had collapsed.

Figure 2.1-11. Approaches to Bridge #3

The sidewalk along the river had an overhanging structure (**Figure 2.1-12**). This overhanging structure, particularly the struts embedded in the concrete, was difficult to inspect.

Figure 2.1-12. Pedestrian deck along river near Bridge #3

(6) Bridge #4: Bekir Karabakak Köprüsü

Bridge #4 was a concrete bridge. Many construction vehicles passed over it (**Figure 2.1-13**).

Figure 2.1-13. Bridge #4

As shown in **Figure 2.1-14**, the girders and shear keys on the upstream side had almost no gap and cracks were developed at the integral part of the girders and piers (left photo). In contrast, the girders and shear keys on the downstream side (right photo) showed a gap. The superstructure may have moved laterally and longitudinally owing to the earthquake. The cracks in the concrete of the girders could be due to the contact of the girders to the shear keys. However, if the pier and the girders were connected with Menase hinge bearings, the cracks could also be due to the spread of the damage along the extension of the Menase hinge reinforcing bars inside the girders.

Figure 2.1-14. Example of damage to Bridge #4

Figure 2.1-15 indicates that the backfill behind the abutment moved forward and subsided.

Figure 2.1-15. Bridge abutment and backfill of Bridge #4

As shown in **Figure 2.1-16**, plants on the bridge turned over and surrounding buildings collapsed.

Figure 2.1-16. Surface of Bridge #4

(7) A bridge seen from Bridge #4 (Figure 2.1-17)

A bridge seen from bridge #4 is a three-span simple girder bridge. The embankment on the side of the right abutment in the photo collapsed. There were concerns about the alignment of the superstructure and damage to the bearings; however, we could not investigate this because of time and schedule constraints. Many construction vehicles used for removing debris passed over it.

Figure 2.1-17. Photos of a bridge taken from Bridge #4

2.1.3. Hatay Airport Road and Hatay Airport

(1) Date and location

The Hatay airport road and the Hatay airport were scanned on March 10, 2023. **Figure 2.1-18** shows their locations.

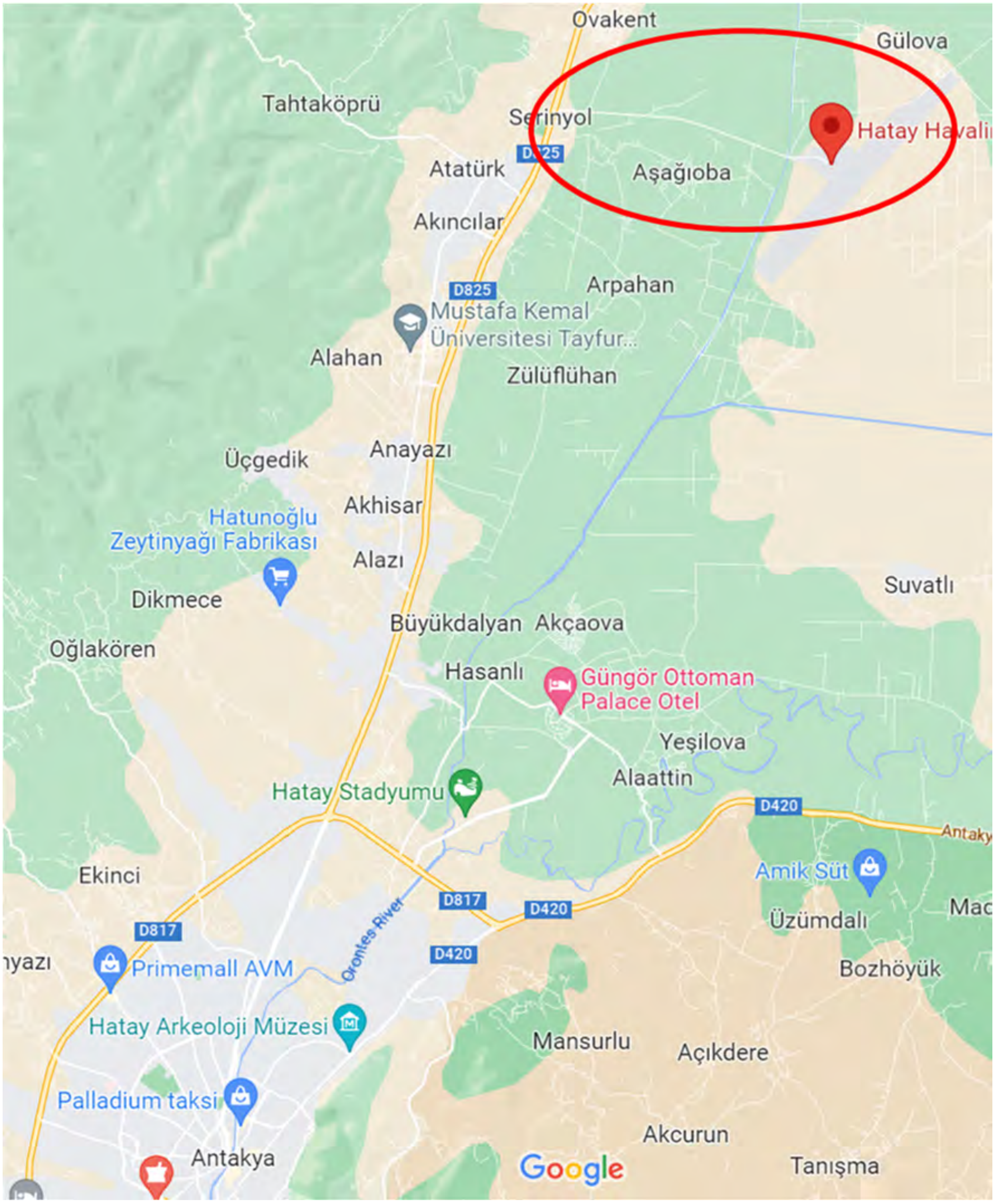

(Made using Google Maps)

Figure 2.1-18. Locations of Hatay airport road and airport

(2) Findings

As shown in **Figure 2.1-19**, the road surface was cracked in several places and certain parts of the road were repaired. A relationship between the road surface cracks and crossing structures such as waterway pipes was supposed; however, no waterway was found within the confirmed range.

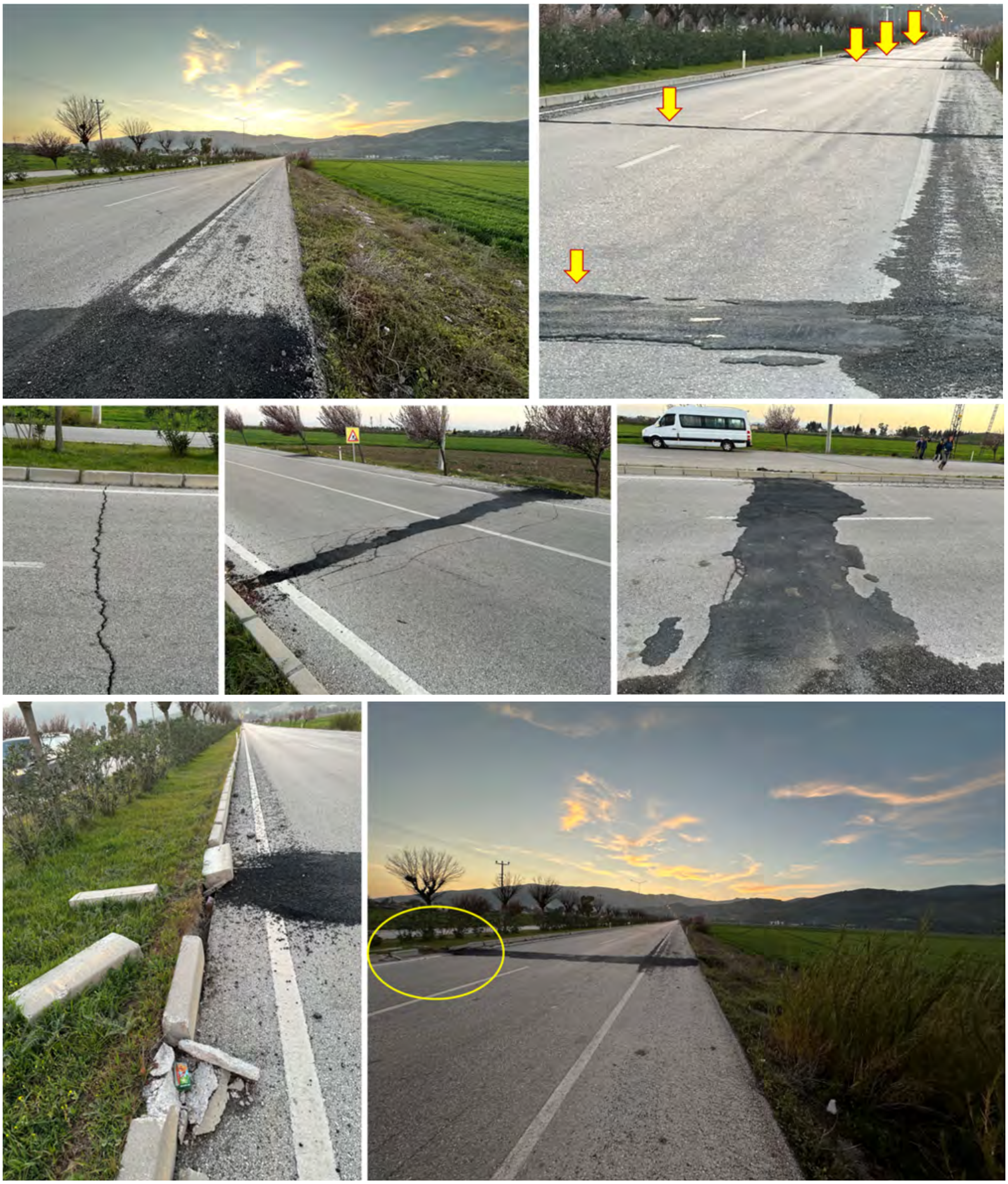

Figure 2.1-19. Cracks on surface of Hatay airport road

As shown in **Figure 2.1-20**, in some places, the pavement was repaired over a relatively wide area. A boring survey was conducted and the cores showed that the subsoil consisted of thick cohesive soil layers.

Figure 2.1-20. Examples of observed damage and boring investigation

Figure 2.1-21 shows that the ground around the Hatay airport terminal building subsided.

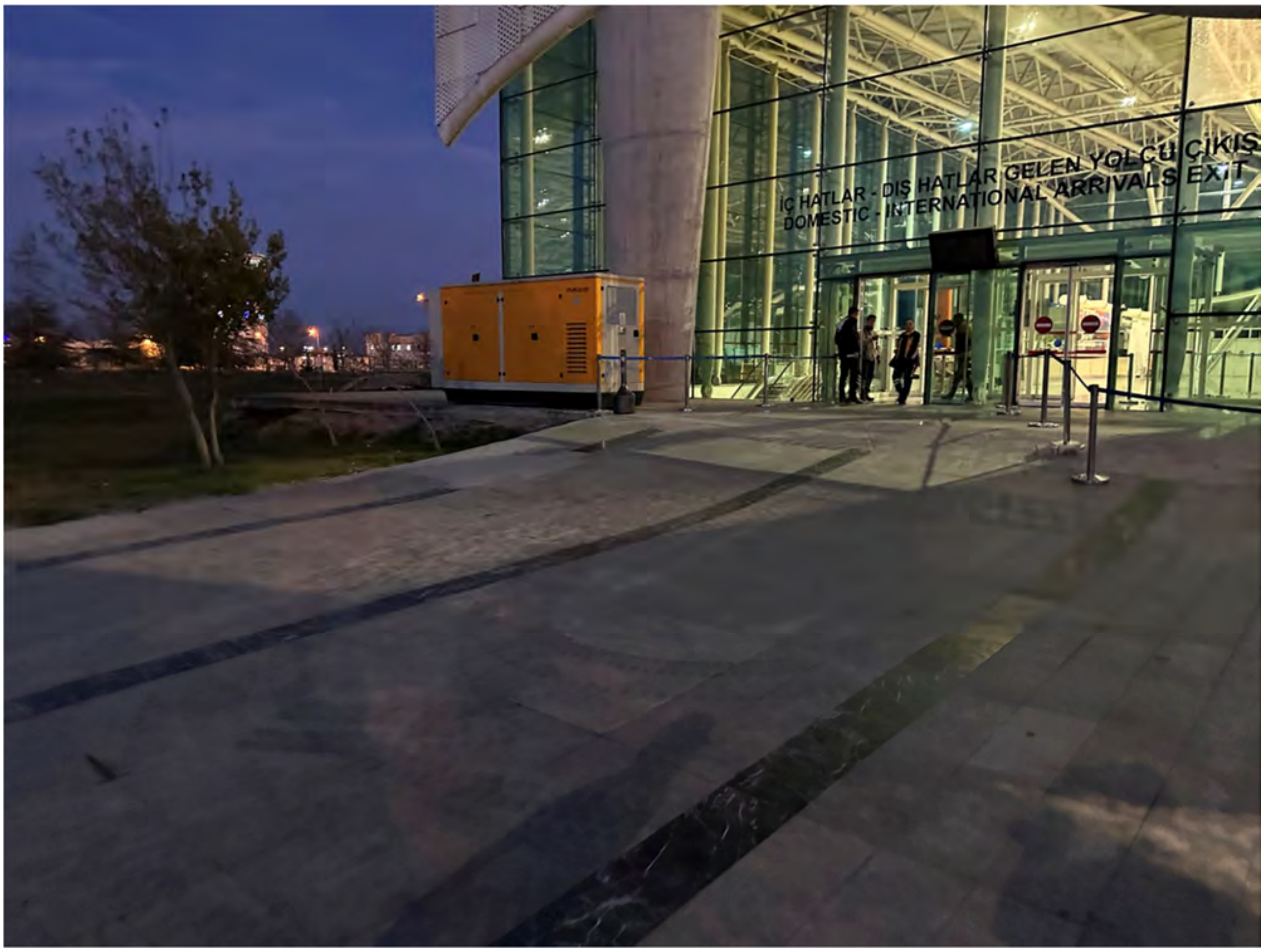

Figure 2.1-21. Slumping of ground surrounding Hatay Airport Terminal building

2.2. Bridge collapse in the suburb of Nurdağı

(1) Date and location

The Nurdağı bridge site was scanned on March 10, 2023. **Figure 2.2-1** shows its location. This bridge crosses D825. During the survey, a road including this bridge was still under construction. For reference, as shown in the right-side photo of **Figure 2.2-1**, N-S-E-W is used to refer to the directions in the explanation hereafter for this bridge.

Figure 2.2-1. Location of collapsed bridge in suburb of Nurdağı (Made using Google Earth)

(2) General view

The bridge spans over the four-lane D825 highway, as shown in **Figure 2.2-2**. As shown in **Figure 2.2-3**, the fallen superstructure was removed and placed on the south side of the western abutment. It is believed to have been a skewed single-span concrete girder bridge.

Figure 2.2-2. Bridge layout

Figure 2.2-3. Abutments and removed girders

(3) Findings

1) East-side abutment

Although the shear key on the left side was destroyed, there was no trace of contact with the girder on the shear key or the parapet on the right side (**Figure 2.2-4**). Scratches on the abutment and spalling of concrete were observed, which were caused when the girders fell off the acute side. Rubber pads were used as a part of the bearings. However, shear keys assumed to have been set between the girders were not observed. Information on whether they were destroyed or did not exist from the beginning was unavailable.

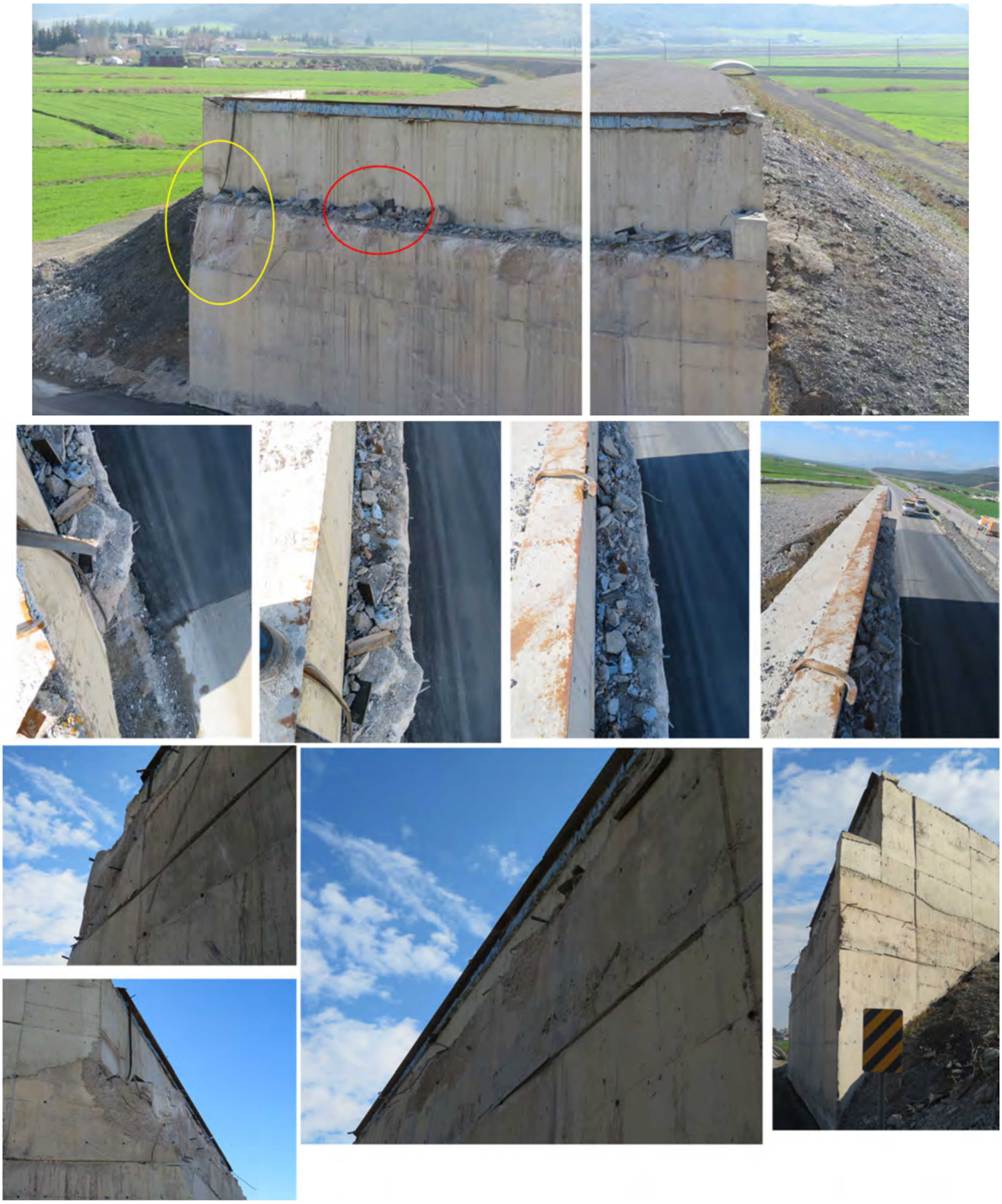

Figure 2.2-4. Observed damage to east-side abutment

2) West-side abutment

Figure 2.2-5 shows that the external shear key on the left side was broken and concrete peeling and rebar exposure were also seen on the same side. Scratches were observed on the front side of the bridge seat. They were considered to be caused by the girders falling off. Although on the right side, scratches, dents, or cracks were not observed on the shear keys, the backwall was damaged. On the bridge seat, concrete blocks considered to be bearing pedestals or shear keys and rubber blocks assumed to be part of the bearings were observed.

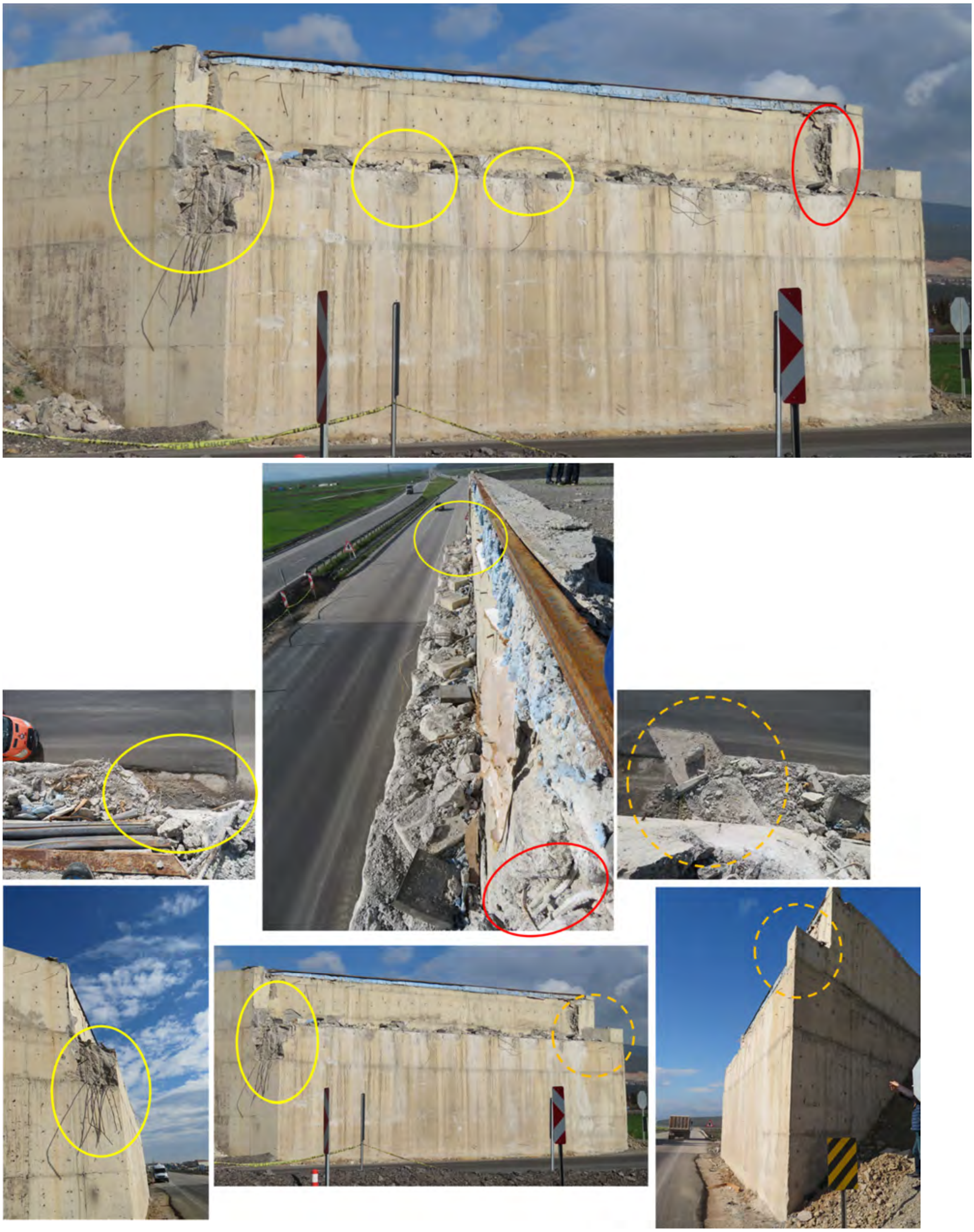

Figure 2.2-5. Observed damage to west-side abutment

3) Comparison of the condition between the east and west-side abutments

Figure 2.2-6 shows that concrete and rubber blocks remained on the west side and appeared to be part of the bearings or the shear keys. However, no information was available on whether they remained in the same condition immediately after the disaster or were affected by the superstructure removal work.

Figure 2.2-6. Comparison of bridge seatings in west and east-side abutments

Figure 2.2-7 shows the measurement results of the seating length and skew angle of the west-side abutment estimated from the photos. The seating length and the skew angle were were approximately 1.1 m and 50°, respectively.

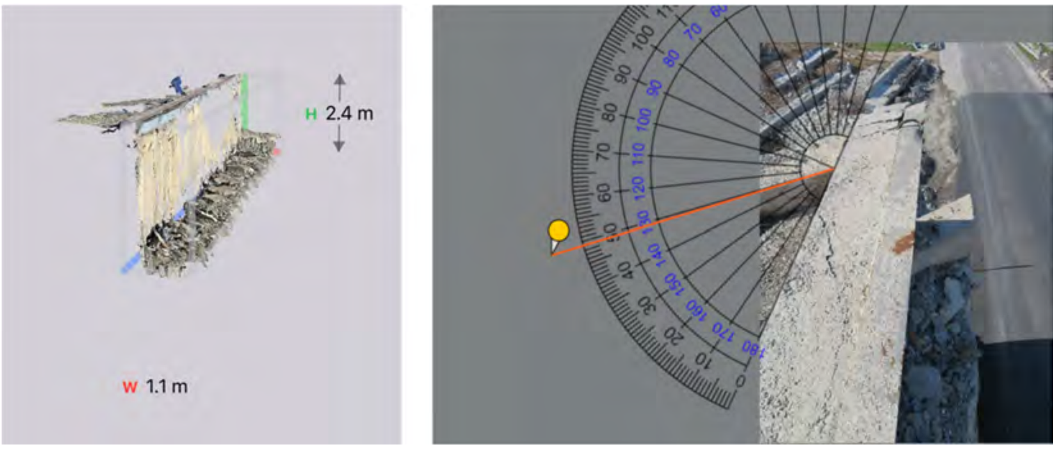

Figure 2.2-7. Measurements of seating length and skew angle

2.3. Tarsus–Adana–Gaziantep motorway (O52) Viaduct between Bahçe and Kömürler toll booths

The following seven bridges on Motorway O52 were surveyed:

1. Motorway O52 Başpınar viaduct
2. Motorway O52 Turgut Özal viaduct
3. Motorway O52 Atatürk viaduct
4. Motorway O52 Nurdağı viaduct
5. Motorway O52 Şehitler viaduct
6. Motorway O52 Kızlaç viaduct
7. Motorway O52 Vecdi Diker viaduct

Figure 2.3-1 shows the locations of the surveyed bridges. Bridges 1–5 are located north of Nurdağı city and close to the fault zone. Bridges 6 and 7 are off the fault zone, and there are mountainous areas between bridges 5 and 6. All bridges were surveyed visually at the ground level under the bridges.

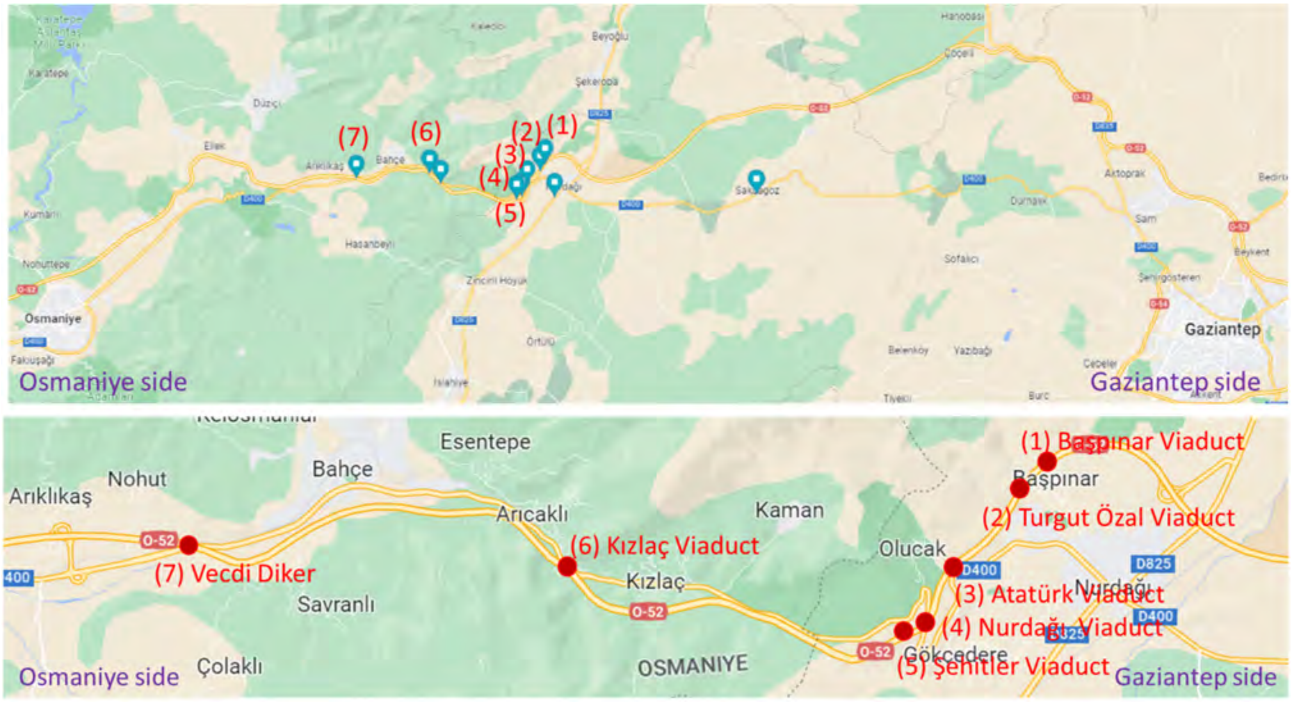

Figure 2.3-1. Locations of bridges surveyed on O52 (Made using Google Maps)

2.3.1. Başpınar Viaduct on Motorway O52

(1) Date and location

The Başpınar viaduct was scanned on March 11, 2023. **Figure 2.3-2** shows the bridge location. A speed limit was imposed on the day the survey was conducted.

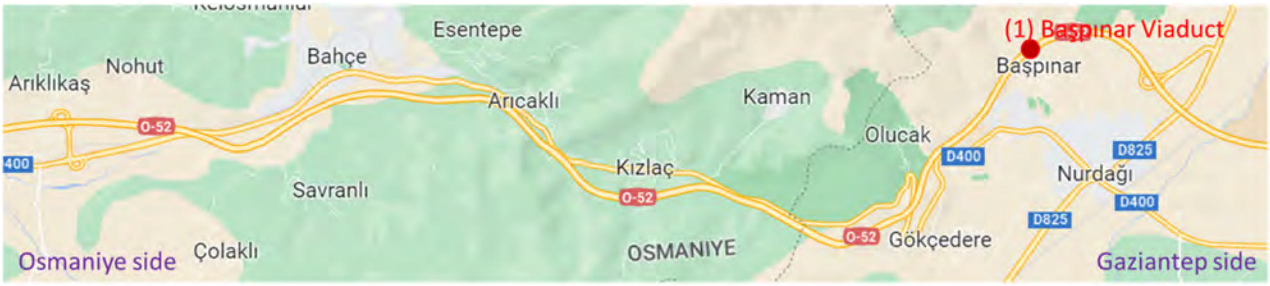

(Made using Google Maps)

Figure 2.3-2. Location of Başpınar viaduct on O52

(2) General view

As shown in **Figure 2.3-3**, the Başpınar viaduct is a multispan bridge with piers of different heights. The superstructure consists of concrete tub girders. The floor slabs appeared continuous through the link slabs, whereas the girders did not. Only the Gaziantep-side half of the bridge was examined.

Figure 2.3-3. Başpınar viaduct on O52

(3) Findings

Figure 2.3-4 shows that the link slabs were damaged. Fallen concrete chunks were observed on the ground.

Figure 2.3-4. Damage to link slabs

Figure 2.3-5 shows an example of minor damage to the surface concrete at the base of high piers in the valley.

Figure 2.3-5. Examples of damage to columns

Figure 2.3-6 shows that the superstructure collided with the abutment. There was a speed limit sign on the bridge.

Figure 2.3-6. Examples of damage due to collision of superstructure and abutment at Gaziantep side

2.3.2. Turgut Özal Viaduct on Motorway O52

(1) Date and location

The Turgut Özal viaduct was scanned on March 11, 2023. A speed restriction was imposed on this bridge on the day the survey was conducted.

(Made using Google Maps)

Figure 2.3-7. Location of Turgut Özal Viaduct on O52

(2) General view

Figure 2.3-8 shows a general view of the bridge. The survey was conducted on the Gaziantep-side half of the bridge. The bridge appeared to be a continuous steel-box girder bridge composed of weathering steel.

Figure 2.3-8. Turgut Özal viaduct on O52

(3) Findings

Figure 2.3-9 shows the surface concrete cracks at the base corners of some piers on the slope.

Figure 2.3-9. Examples of damage to column bases

As shown in **Figure 2.3-10**, cracks were present in the pavement behind the Gaziantep-side abutment. The parapet wall was misaligned over the expansion joint. In addition, cylindrical members installed between the girders and the parapet were damaged. This is considered to have prevented the girders from directly colliding with the abutment.

Figure 2.3-10. Examples of damage observed around Gaziantep-side abutment

As shown in **Figure 2.3-11**, there were contact marks on the concrete blocks of the abutment where the lateral stopper was installed on the underside of the lower flange of the box girder and was considered to have collided during the earthquake. Conversely, no contact traces were observed between the steel cantilever stopper installed on the abutment seat adhering to the girder web, which was considered to sandwich the superstructure to prevent it from falling laterally. However, it was unclear whether the lateral steel stopper under the superstructure and the steel cantilever stopper on the side were designed to work together or whether one of them was supposed to act as a backup after the other failed.

Figure 2.3-11. Lateral stopper below lower flange of box girder

Figure 2.3-12 shows a bearing on the abutment. The type of bearing support used was uncertain. No apparent trace of sliding displacement of the bearing was observed.

Figure 2.3-12. Bearing support on abutment

Figure 2.3-13 shows the arrangement of the structural parts around the pier bearings. Concrete blocks were arranged. Displacement-restraining steel cantilevers were placed on the seat, which can support the side of the box girder web in case. Cylindrical parts were placed underneath the steel box girder. It was unclear how these three parts, namely, the concrete blocks, steel cantilevers, and cylindrical parts, worked together to prevent excessive girder movement in the longitudinal or perpendicular direction to the bridge axis.

Figure 2.3-13. Arrangement of structural parts on piers

2.3.3. Atatürk Viaduct on Motorway O52

(1) Date and location

The Atatürk viaduct was scanned on March 11, 2023.

(Made using Google Maps)

Figure 2.3-14. Location of Atatürk viaduct on O52

(2) General view

Figure 2.3-15 shows the Atatürk viaduct location. It was extremely high to check the structural details; however, the girder system, columns, bearings, and their surrounding components appeared similar to those of the Turgut Özal viaduct.

Figure 2.3-15. Atatürk viaduct on motorway O52

(3) Findings

The base of a pier in the valley was investigated. **Figure 2.3-16** shows concrete delamination at the base of the pier. Assuming the bridge structure is similar to the Turgut Özal viaduct structure, the shock absorbers connecting the girders and the abutment and the lateral stoppers below the lower flange of the box girder could be damaged as in the Turgut Özal viaduct. However, the Atatürk viaduct was extremely high to approach and investigate these components. Because the superstructure is supported by piers of considerably different heights, the bridge behavior could be complex. Therefore, it would be interesting to check how the bridge behaved and whether the displacements at the flexible columns, abutments, sliding bearings, and material serving as shock absorbers were balanced in the calculation.

Figure 2.3-16. Examples of damage to column bases

(4) Remarks

As shown in **Figure 2.3-17**, at the time of the survey, the road surface of National Highway D400, which is parallel to the pier location of the Atatürk viaduct, was being repaired.

Figure 2.3-17. Repair of National Highway D400 near Atatürk viaduct

2.3.4. Nurdağı Viaduct on Motorway O52

(1) Date and location

The Nurdağı viaduct was scanned on March 11, 2023.

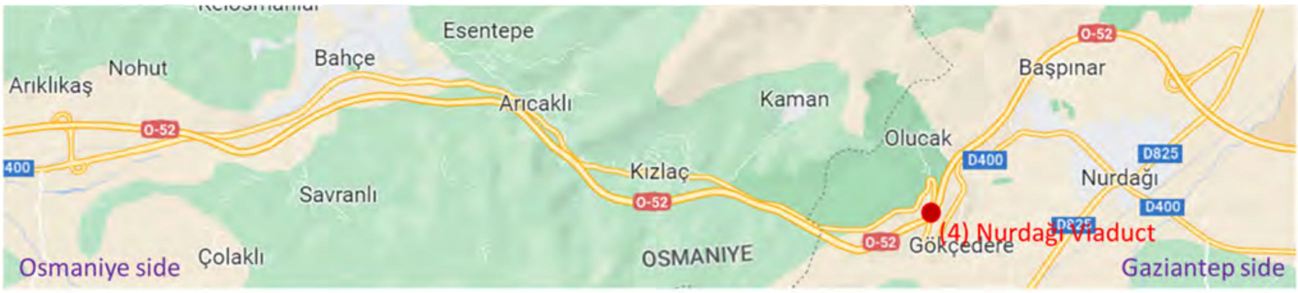

(Made using Google Maps)

Figure 2.3-18. Location of Nurdağı viaduct on motorway O52

(2) General view

Figure 2.3-19 shows a general view of the Nurdağı Viaduct. The viaduct is separated in different directions. The bridge towards Gaziantep was in service and was temporarily switched to two-way lanes at the time of the survey. The other bridge towards Osmaniye was closed to traffic, and expansion joint replacement work was underway. Both superstructures consist of steel-box girder and prestressed concrete (PC) tub girder sections. The steel-box sections were considered continuous, and the PC tub girder sections were assumed to be connected via link slabs.

Figure 2.3-19. Nurdağı viaduct on O52

(3) Findings

Figure 2.3-20 shows the abutment and the neighboring column supporting the closed superstructure. During the survey, expansion joint replacement of the abutment was underway. Concrete fell off from the block underneath the link slab with exposed rebars. From the long-distance observation, it was unclear if the girder end was damaged.

Figure 2.3-20. Expansion joint replacement work on Gaziantep-side abutment and concrete block to support link slab on column next to abutment on closed side of bridge.

As shown in **Figure 2.3-21**, on the closed side of the bridge, the superstructure transitioned from a concrete girder to a steel-box girder on the second pier from the Gaziantep-side abutment. The pier was damaged in the middle and the base. Particularly in the middle part, the surface and a part of the core concrete fell off, and the longitudinal rebars deformed, indicating a significant decrease in the shear and bending strengths. The photo also shows double hoop bars arranged inside. The bridge surface also appeared to be distressed above the same pier.

Figure 2.3-21. Severe damage to column supporting transition section from concrete girder to steel-box girder on closed side of bridge

Figure 2.3-22 shows a photograph of the abutment on the Gaziantep side taken from under the bridge, viewing at the girder ends. This was the in-service side of the bridge. The expansion joint was considered to be damaged, even on the in-service side of the bridge, because the photos showed damage to the backwall near the expansion joint.

Figure 2.3-22. Gaziantep-side abutment on in-service side of bridge

Figure 2.3-23 shows the condition of the abutments on the Osmaniye side. The photos on the left and right show the girder on the in-service and closed sides of the bridge, respectively. The photograph on the left-hand side shows concrete debris accumulated on the bridge seating, that is, the in-service side of the bridge. This indicates that the expansion joint collapsed because of the collision of the box girder with the abutment during the earthquake.

Figure 2.3-23. Abutments on Osmaniye side: Left = in-service side of bridge, Right = closed side of bridge

Figure 2.3-24 shows the surroundings of the bearings on the in-service side of the bridge. The bottom flange buckled above the bearings. In addition, the covers of the bearings were deformed, indicating bearing damage. **Figure 2.3-24** also indicates that the bearings could have been subjected to a large force during the earthquake and were probably deformed based on the deformation of the bearing cover and the girders. Additionally, no unseating prevention devices for failure safety were noticeable on the bridge.

Figure 2.3-24. Local buckling of bottom flange above bearing on in-service side of bridge

2.3.5. Şehitler Viaduct on Motorway O52

(1) Date and location

The Şehitler viaduct was scanned on March 11, 2023.

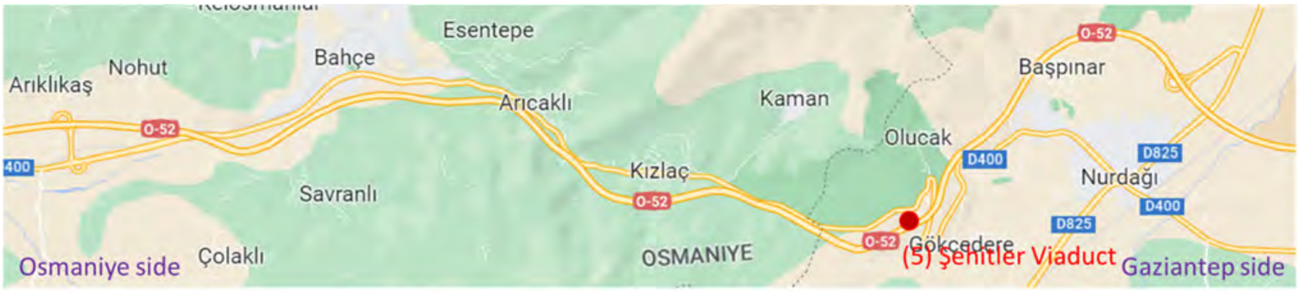

(Made using Google Maps)

Figure 2.3-25. Location of Şehitler viaduct on O52

(2) General view

Figure 2.3-26 shows a general view of the bridge. The bridge structure is similar to that of the Başpınar viaduct. **Figure 2.3-26** also shows that, during the survey, earthwork was underway at the base of the valley under the bridge center span.

Figure 2.3-26. Şehitler viaduct on O52

(3) Findings

As shown in **Figure 2.3-27**, at the time of the survey, construction work was underway at the bottom of the valley. The ground level was considered to differ after the earthquake because of traits and stains of soil on the piers and shot concrete on the surrounding cut slope. The aim of construction work was not sure but it could be to fill the soil movement around the piers caused during the earthquake.

Figure 2.3-27. Grounds surrounding bridge piers

As shown in **Figure 2.3-28**, one of the piers was approachable and minor cracks were observed.

Figure 2.3-28. Horizontal crack in bridge column

Figure 2.3-29 shows that the superstructure collided with the abutment during the earthquake, which was also observed for the Başpınar viaduct. Damage to the link slabs was also observed.

Figure 2.3-29. Examples of damage to expansion joint and link slabs

2.3.6. Kızlaç Viaduct on Motorway O52

(1) Date and location

The Kızlaç viaduct was scanned on March 11, 2023. The bridge runs parallel to D400, as shown in **Figure 2.3-30**.

(Made using Google Maps)

Figure 2.3-30. Location of Kızlaç viaduct on O52

(2) General view

The viaduct is adjacent to a tunnel, as shown in **Figure 2.3-31**. As shown in **Figures 2.3-31** and **2.3-32,** the bridge has continuous steel-box and PC tub girder sections. Weathering steel is used for the steel-box girders. Separate bridges run parallel along D400 and the foot of the mountains.

Figure 2.3-31. Kızlaç viaduct on O52

Figure 2.3-32. Girder–column connections

(3) Findings

As shown in **Figure 2.3-33**, no distress was observed on the road surface above the Gaziantep-side abutment. A lateral displacement restrainer adhering to the bottom flange and sandwiched between two concrete blocks is present, with the concrete blocks also functioning as bearing pedestals. There was no indication of the lateral displacement restrainer having collided with the concrete blocks. The bearings on the concrete blocks exhibited no residual deformation.

Figure 2.3-33. Photographs of expansion joint, bearing, and lateral displacement restrainer on Gaziantep-side abutment on mountain-side bridge

The clearance under the girder is very narrow on the Gaziantep side of the bridge. As shown in **Figure 2.3-34**, nonuniform rust developed in the weathering steel near the observed girder end.

Figure 2.3-34. Nonuniform rust development in weathering steel girder

Figure 2.3-35 shows the bearings and lateral displacement restrainer on the first column from the Gaziantep-side abutment. The column is very short and resembles a slab. The bearings are surrounded by steel cages. There are no traces of contact between the lateral displacement restrainer and the concrete blocks.

Figure 2.3-35. Horizontal displacement restrainer of girder and concrete blocks on column next to Gaziantep-side abutment

Figure 2.3-36 shows the girder end near the Gaziantep-side abutment of the D400-side bridge. The superstructure details are the same as those of the mountain-side superstructure and nonuniform rust is not observed in the weathering steel. This could be attributed to the wider clearance between the girder bottom and the ground compared to that in the mountain-side superstructure.

Figure 2.3-36. Superstructure and Gaziantep-side abutment on D400-side bridge

Figure 2.3-37 shows the expansion joint and the road surface behind the tunnel-side (or Osmaniye-side) abutment on the mountain-side bridge. The plates in the transition section of the parapet walls above the expansion joint between the bridge and backfill were deformed. The pavement behind the abutment appeared to have been repaired after the earthquake on both the mountain- and D400-side bridges. As shown in **Figure 2.3-38**, the shear keys were in contact with the adjacent girders; however, the superstructure did not appear to be offset to the left or right.

Figure 2.3-37. Deformed plates in transition section of parapet walls between bridge and backfill sections

Figure 2.3-38. Tub girders, shear keys, and bearings

Minor horizontal cracks were observed in some piers, as shown in **Figure 2.3-39**.

Figure 2.3-39. Horizontal crack in column

(4) Note

Figure 2.3-40 shows the neighboring roads and buildings. No notable collapse was observed. The bridge area was located over mountains from Nurdağı, and the scale of the seismic ground motion was possibly much smaller than that of the Nurdağı area.

Figure 2.3-40. Roads and buildings around viaduct

2.3.7. Vecdi Diker Viaduct on Motorway O52

(1) Date and location

The Vecdi Diker viaduct was scanned on March 11, 2023.

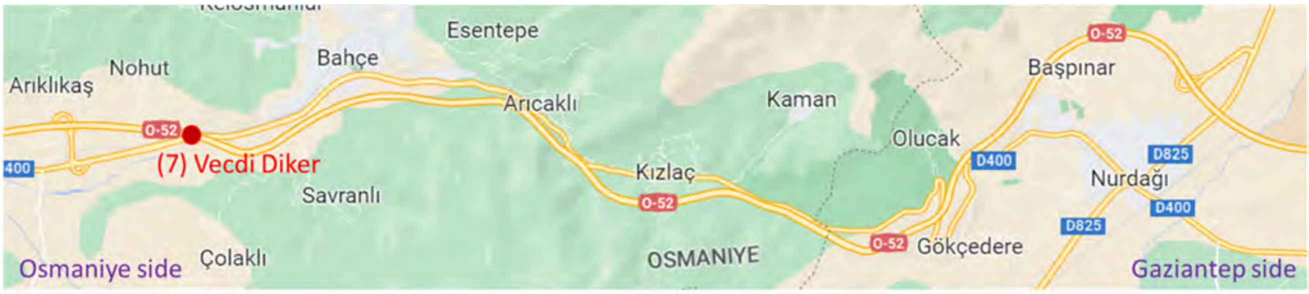

(Made using Google Maps)

Figure 2.3-41. Location of Vecdi Diker viaduct on O52

(2) General view

As shown in **Figure 2.3-42**, two bridges toward Gaziantep and Osmaniye are adjacent to each other. They are continuous steel-box girder bridges crossing a channel, road, and railway. Seismic dampers are installed in the first column from the abutments at both ends and connected from the column to the girder.

Figure 2.3-42. Vecdi Diker viaduct on O52

(3) Findings

Figure 2.3-43 shows photographs of the dampers. No traits or signs indicated that the dampers functioned during the earthquake. Some bearings were covered with a black sheet, whereas others lost their covers.

Figure 2.3-43. Dampers of Vecdi Diker viaduct

As shown in **Figure 2.3-44**, the bearings are protected by cylindrical metallic covers. Some metallic covers were deformed, and black objects protruded internally from the metallic covers. These observations indicated that the bearings suffered large displacements, and therefore, the conditions of all bearings of this bridge must be checked.

Figure 2.3-44. Examples of observed damage to bearing covers

2.4. Damage to earthworks, a tunnel, and bridges on national highways connecting Gaziantep and Malatya

Figure 2.4-1 shows the locations of the following surveyed earthworks, tunnel, and two bridges:

1. The section along the Göksu river on the D850 Malatya/Kahramanmaraş highway,
2. The Erkenek tunnel on the D850 Malatya/Kahramanmaraş highway,
3. The Beylerderesi Turgut Özal viaduct on the D850 Malatya/Kahramanmaraş highway, and
4. The Thoma bridge on the D875 Malatya/Keban highway.

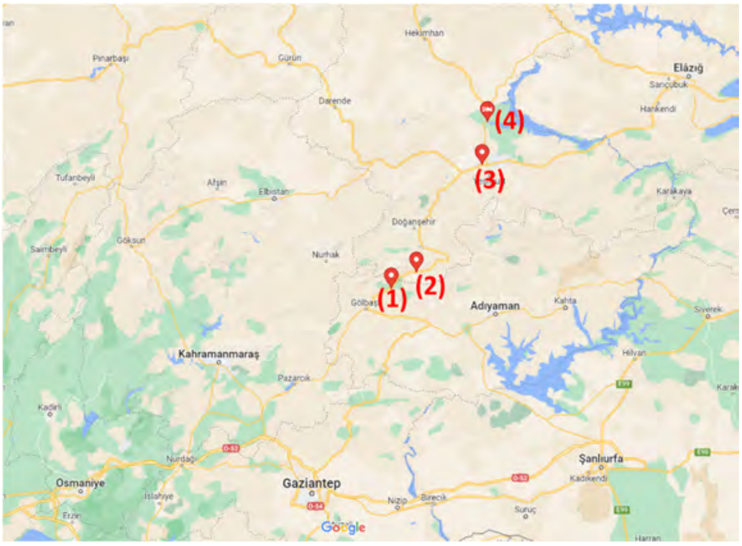

Figure 2.4-1. Surveyed locations (Made using Google Maps)

2.4.1. Section along the Göksu River on D850 Malatya/Kahramanmaraş Highway

(1) Date and location

The Göksu river was surveyed on March 12, 2023. This section runs along a small dam.


Figure 2.4-2. Location of surveyed section on D850 along Göksu river (Made using Google Earth)

(2) Findings

As shown in **Figure 2.4-3**, the surveyed section is a four-lane road, with the two lanes on the mountainside under repair and the other two in service.

Figure 2.4-3. Examples of observed damage to road embankments

As shown in **Figure 2.4-4**, an old road was observed on the mountainside whose parts had collapsed.

Figure 2.4-4. Damage to retaining walls

Cut-slope failure with the collapse of the retaining wall was also observed, as shown in **Figure 2.4-5**.

Figure 2.4-5. Cut-slope failure with collapse of retaining wall

2.4.2. Erkenek Tunnel on D850 Malatya/Kahramanmaraş Highway

(1) Date and location

The Erkenek tunnel was surveyed on March 12, 2023. The tunnel location is shown in **Figure 2.4-6**.

(Made using Google Earth)

Figure 2.4-6. Location of Erkenek tunnel on D850 Malatya/Kahramanmaraş highway

(2) Findings

As shown in **Figure 2.4-7**, at the time of the survey, the northbound tunnel (the tunnel on the left side in the photo) was closed to traffic and the southbound tunnel was used for two-lane traffic facing each other. The tunnel operation office is located near the tunnel.

Figure 2.4-7. Erkenek tunnel on D850 and operation office

Figure 2.4-8 shows examples of CCTV camera images of the northbound tunnel. Traffic was closed for safety reasons, and entry into the tunnel was not allowed. In the tunnel, cracks were observed on the road surface in the longitudinal direction. In addition, the fallen concrete debris was being removed from the tunnel.

Figure 2.4-8. CCTV camera images of clearing work in Erkenek tunnel

Traffic was not allowed to enter the north tunnel. The south tunnel was open to traffic; however, there was a notable traffic safety concern for pedestrians because there were no sidewalks or decent shoulders in the tunnel. Accordingly, a video of the interior of the south tunnel was recorded from a car. **Figure 2.4-9** shows the damaged state inside the tunnel. The lining concrete had large cracks on its sides and top, and in some places the concrete blocks were probable to fall. This damage was similar to that observed during the 2004 Niigata Chuetsu Earthquake (Konagai et al., 2005; NILIM/PWRI, 2005a; NILIM/PWRI, 2005b) and the 2016 Kumamoto Earthquake (Fukuhara and Nakahara, 2018; NILIM/PWRI, 2017) in Japan. Given the location and direction of the lining damage, the lining concrete was subjected to complex stress conditions owing to the possible inward forces caused by the movement of the surrounding soil and rock toward the lining. Jet fans and information boards were anchored to the concrete lining; however, the condition of the concrete near the anchors could not be confirmed from the video.

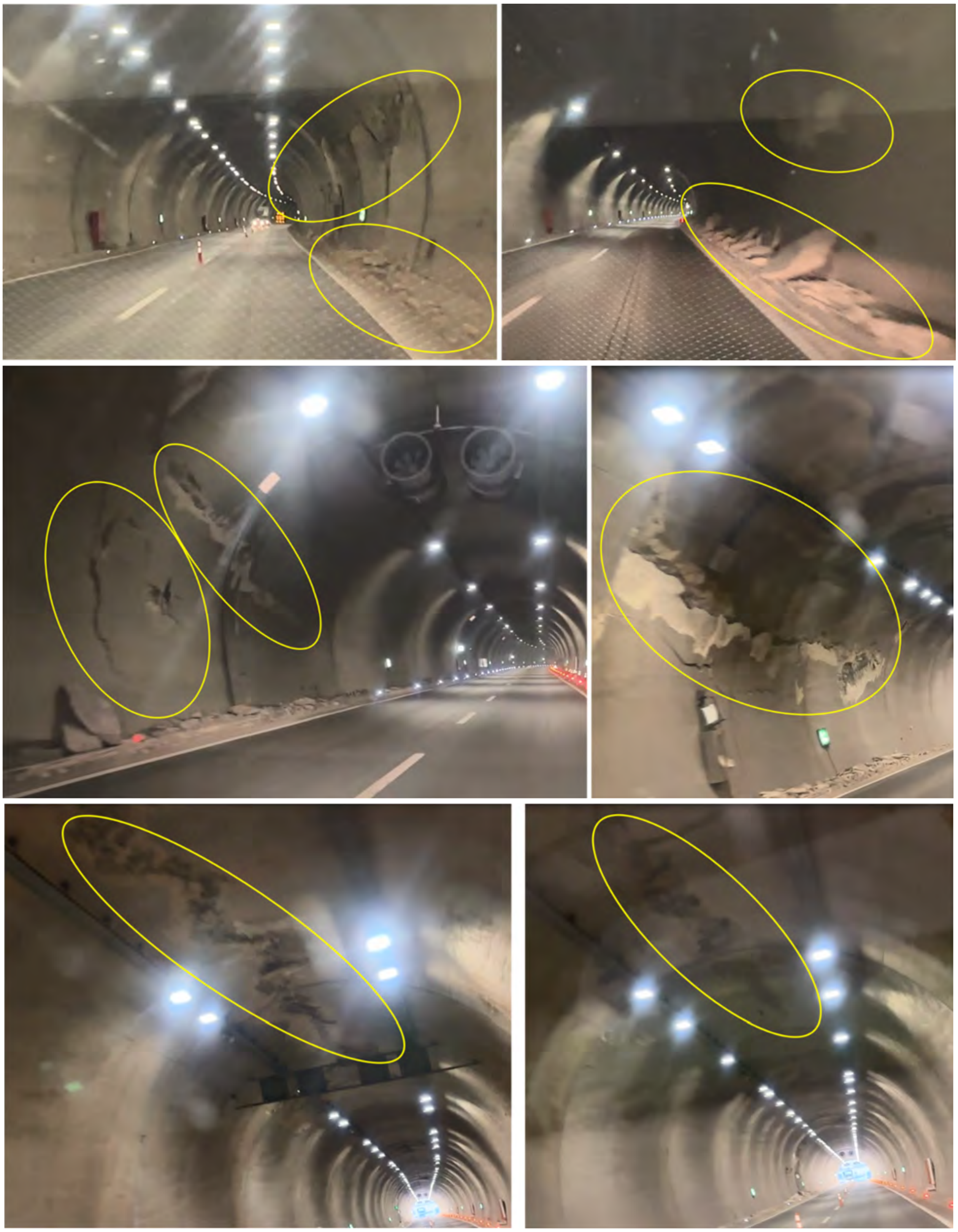

Figure 2.4-9. Examples of observed damage to Erkenek tunnel

(4) Remarks

Figure 2.4-10 shows a rock shed adjacent to the Erkenek tunnel. No particular damage was found from the moving-vehicle observations.

Figure 2.4-10. Rock shed adjacent to Erkenek tunnel

2.4.3. Beylerderesi Turgut Özal Viaduct on D850 Malatya/Kahramanmaraş Highway

(1) Date and location

The Beylerderesi Turgut Özal viaduct was scanned on March 12, 2023.

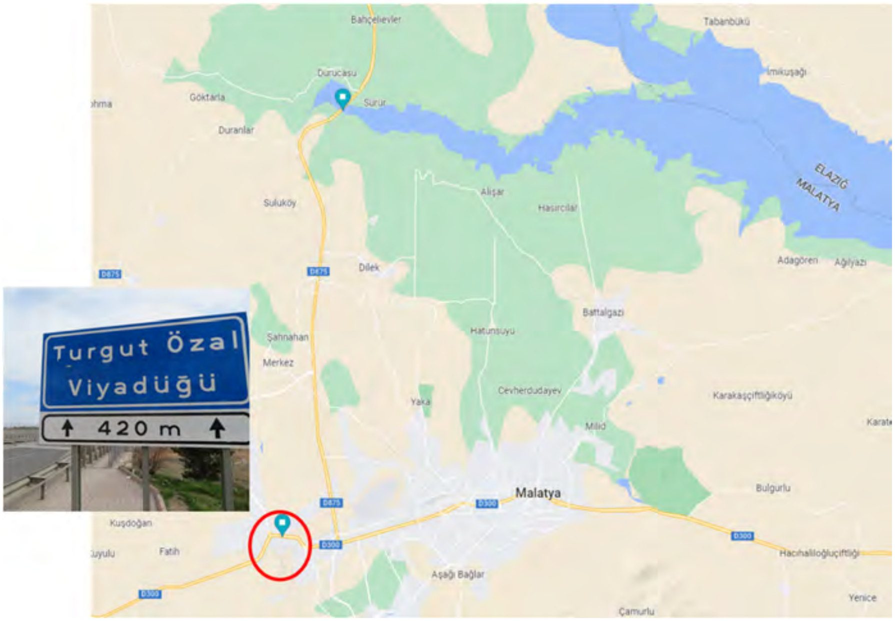

(Made using Google Maps)

Figure 2.4-11. Location of Beylerderesi Turgut Özal viaduct on D850 Malatya/Kahramanmaraş highway

(2) General view

The bridge is located downstream of the Yeşilvadi (Beylerderesi) dam. **Figure 2.4-12** shows a general view of the bridge. The bridge is a balanced cantilever concrete box-girder bridge.

Figure 2.4-12. Beylerderesi Turgut Özal viaduct on D850 (E and W denote the east and west sides of bridge, respectively, in photos)

As shown in **Figure 2.4-13**, an outer cable system is installed. **Figure 2.4-13** also shows the center span sagging toward the middle part.

Figure 2.4-13. Center span sagging and outer cable system

(3) Findings

Figure 2.3-14 shows the eastern abutment. A rubber cover surrounds each bearing. The centerlines of the bearings and the bearing pedestal concrete did not match; however, it was uncertain whether the girder moved forward during the earthquake.

Figure 2.4-14. East-side abutment

Figure 2.4-15 shows the damage around the west-side abutment. The damage indicated that the girder and the abutment collided.

Figure 2.4-15. Examples of observed damage to girder-end and west-side abutment

As shown in **Figure 2.4-16**, the shear key concrete was damaged, indicating that the bridge was heavily shaken in a direction perpendicular to the bridge axis. The Styrofoam under the shear key was torn apart and fell to the ground in front of the abutment. The front face of the shear key was also positioned forward compared with the front surface of the abutment.

Figure 2.4-16. Examples of observed damage to shear key on west-side abutment.

As shown in **Figure 2.4-17**, vinyl and metal covers surrounded the bearings, hindering their inspection.

Figure 2.4-17. Bearings and their covers

Figure 2.4-18 shows the east-side pier. A slope was behind the east-side pier and falling rocks were observed around the pier, indicating that some reached the pier during the earthquake. A frame was fixed to the pier and maintained its shape. As shown in **Figure 2.4-19**, no dents or cracks were observed in the column.

Figure 2.4-18. East-side pier and fallen rocks

Figure 2.4-19. Base of east-side pier

Figure 2.4-20 shows the western pier. A few small fallen rocks were observed around the western pier. No damage was observed on the pier, as shown in **Figure 2.4-21**.

Figure 2.4-20. West-side pier and fallen debris around it

Figure 2.4-21. Base of west-side pier

(4) Remarks

Figure 2.4-22 shows the Beylerderesi dam. No cracks, leaks, or other distresses were observed in the dam.

Figure 2.4-22. Beylerderesi dam and surrounding ground

2.4.4. Tohma Bridge on D875 Malatya/Keban Highway

(1) Date and location

The Tohma bridge was scanned on March 12, 2023. This bridge crosses the Karakaya dam, as shown in **Figure 2.4-23**.

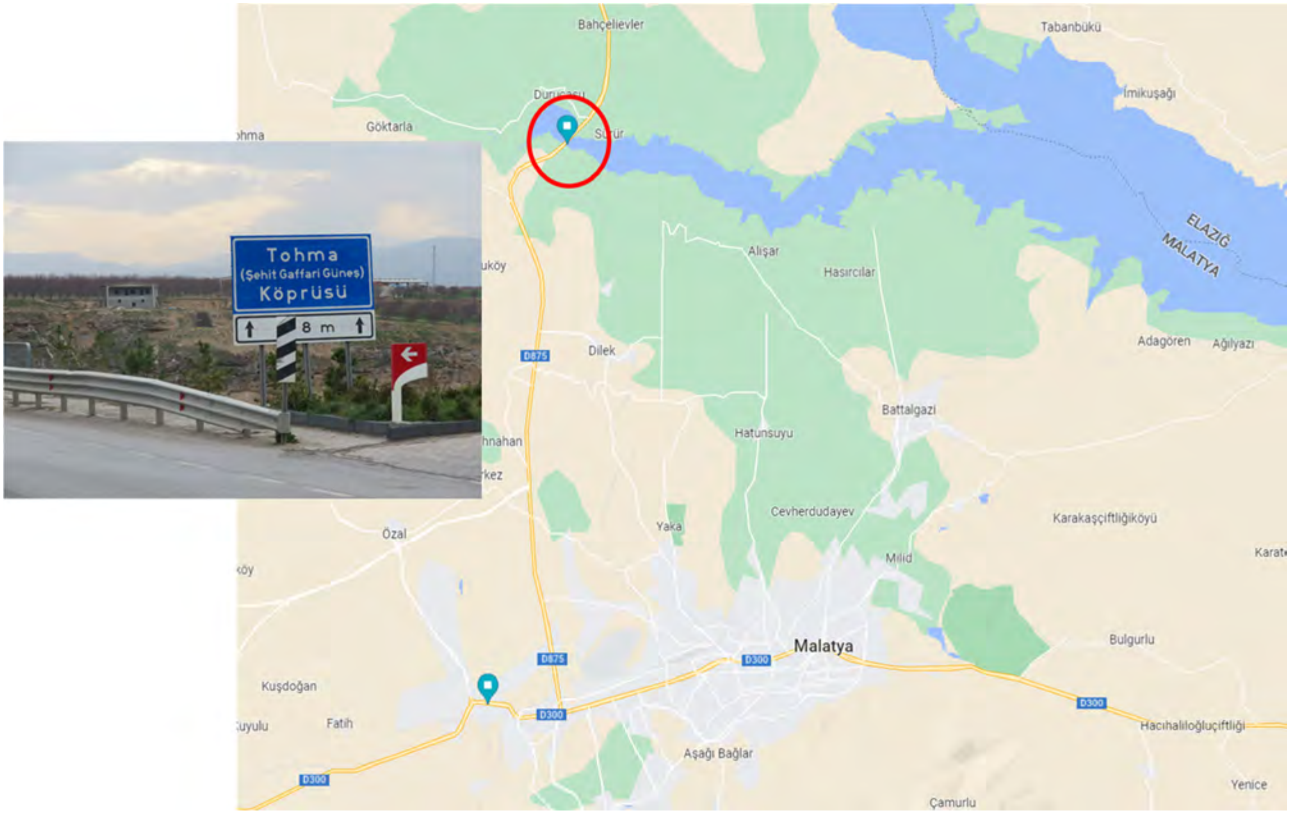

(Made using Google Maps)

Figure 2.4-23. Location of Tohma bridge on D875 Malatya/Keban highway

(2) General view

Figure 2.4-24 shows the Tohma bridge. The bridge comprises of old and new bridges. The old bridge consists of railroad and northbound road superstructures. Both bridges are concrete girder bridges. The southbound bridge is a steel girder bridge. The piers are located in a wetland. A train passed during the investigation; however, it was slow. Traits that looked like sand boils were observed on the ground surface near this bridge; however, it was unclear what they were because we did not approach them.

Figure 2.4-24. Tohma bridge on D875 Malatya/Keban highway

(3) Findings

Figure 2.4-25 shows the road surface around the south-side (Malatya-side) abutment. The bridge collided with the abutment, and the superstructure and the abutment were dislocated from each other in a perpendicular direction to the bridge axis.

Figure 2.4-25. Examples of damage around south-side abutment

As shown in **Figure 2.4-26**–**Figure 2.4-28**, dampers were installed behind each steel girder of the new bridge; however, they were disconnected. The threads of the screw connections of the dampers were not stripped and the screw connections exhibited rust.

Figure 2.4-26. Damage to dampers

Figure 2.4-27. Connection parts of dampers

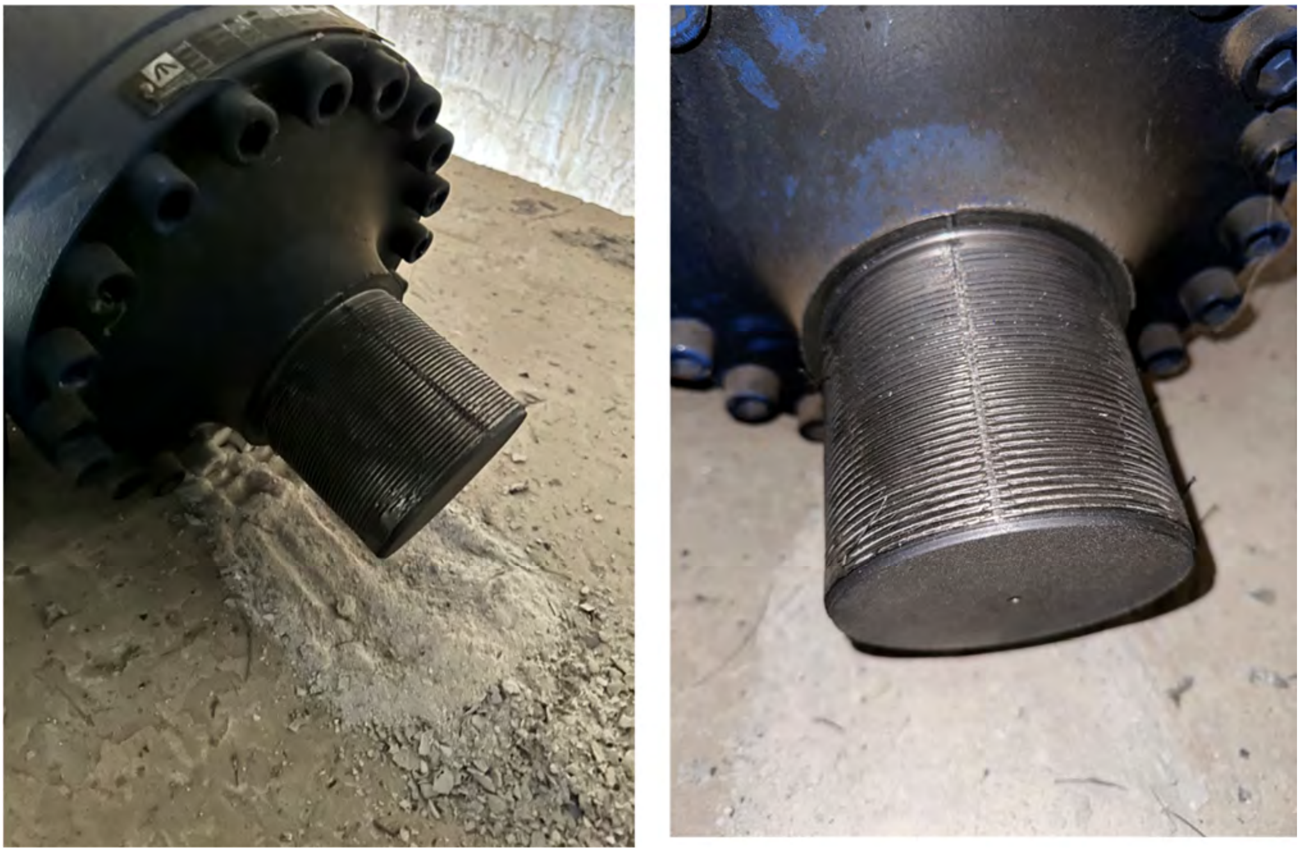

Figure 2.4-28. Connection screw parts of dampers

Figure 2.4-29 shows the old bridge had large cracks in the abutment backwall and the cover concrete ripped off over a wide range. This indicated that the concrete girder collided with the backwall during the earthquake. In addition, the shear keys on the abutment collapsed because of a collision with the adjacent beam.

Figure 2.4-29. Examples of damage to abutment parapet wall and shear keys

Figure 2.4-30 shows a photo of the seating of the pier of the old bridge, as seen from the abutment. The shear keys of the road girders were damaged, indicating that the superstructure had moved horizontally. **Figure 2.4-31** shows the seating of the pier of the new bridge, which was also seen from the abutment. Based on the distant view, it was unclear whether there was damage, but cracks appeared to develop at the bases of the shear keys.

Figure 2.4-30. Damage to shear keys on pier of old bridge

Figure 2.4-31. Damage to shear keys on pier of new bridge

The bridge surface was examined on foot. The floor slab was not continuous over the piers, and expansion joints were present between the spans. As shown in **Figure 2.4-32**, the superstructures were displaced from each other over the piers. Damage to the bearings and girder ends was presumed. Although inspection is necessary, the structure is not designed to allow easy access to the bearings. For example, no inspection facility was available for the superstructures. The superstructures were extremely close to each other horizontally to operate the inspection platform of a bridge inspection truck between them. As shown in **Figure 2.4-33**, soil deformation (cracking) was also observed around some piers.

Figure 2.4-32. Dislocation of spans from each other over piers

Figure 2.4-33. Dislocation of spans from each other over piers and cracks on ground surface

Figure 2.4-34 shows the north-side (Elâzığ-side) abutment of the new bridge. The pavement behind the old bridge was repaired. The abutment concrete fell off and the anchor bolts of the lighting pole foundation were exposed. The girder and the abutment appeared to have collided with each other.

Figure 2.4-34. Northern (Elâzığ-side) abutment

Figure 2.4-35 shows close-up views of the north-side abutments. No damage to the abutments of the new bridge was observed. In the new bridge, jigs were installed on the girders and the abutments. Installation of attachments to prevent the bridge from unseating seemed to be planned.

Figure 2.4-35. Close-up views of north-side abutments

However, as shown in **Figure 2.4-36**, dampers were installed to connect each steel girder to the north-side abutment in the new bridge, as they were at the south-side abutment. They looked intact. A photo of one of the bearings on the abutment is shown in **Figure 2.4-36**, indicating no evidence of movement during the earthquake.

Figure 2.4-36. Dampers and bearings in north-side abutment of new bridge

Figure 2.4-37 shows the bearings on the piers neighboring the north-side abutment of the new bridge. The bearings on the piers appear to be the same as those on the abutment. Based on the photo, the bottom flange of the girder was deformed; however, this was not certain.

Figure 2.4-37. Bearings on piers of new bridge

Figure 2.4-38 shows photos of the pier caps captured from the abutment. Based on these photos, it is uncertain that the girders and the shear keys were in contact with each other in the road bridges during the earthquake, whereas some shear keys were damaged in the railway bridge.

Figure 2.4-38. Shear keys on pier caps

The soil was considered to have subsided around some footings, as shown in **Figure 2.4-39**. Because the footings were extremely deep to climb, it was impossible to approach the bases of the piers. Photos taken from a distance indicated no significant damage, as **Figure 2.4-39** also shows.

Figure 2.4-39. Bases of some piers and surrounding ground surface

(4) Remarks

Figure 2.4-40 shows photos of the deck slabs. There were white stains on the deck slabs, and, accordingly, the cause of these stains should be checked from the viewpoint of durability of the deck concrete.

Figure 2.4-40. Deck slabs of new bridge

2.5. Examples of other noteworthy observations

2.5.1. Roads in downtown Antakya city

During the survey, electric poles were rarely observed in Turkey, as shown in **Figure 2.5-1**.

Figure 2.5-1. Examples of observed damage to buildings and road ancillaries in downtown Antakya city

2.5.2. Suburban roads of Antakya city

Figure 2.5-2 shows examples of rockfalls on a road in suburban Antakya. Because it was a four-lane road, the fallen rocks did not block all the lanes.

Figure 2.5-2. Rockfalls in suburban Antakya

2.5.3. D400 section near Sakcagoz between Gaziantep and Nurdağı

Figure 2.5-3 shows the location of Sakcagoz. It lies between Nurdağı and Gaziantep.

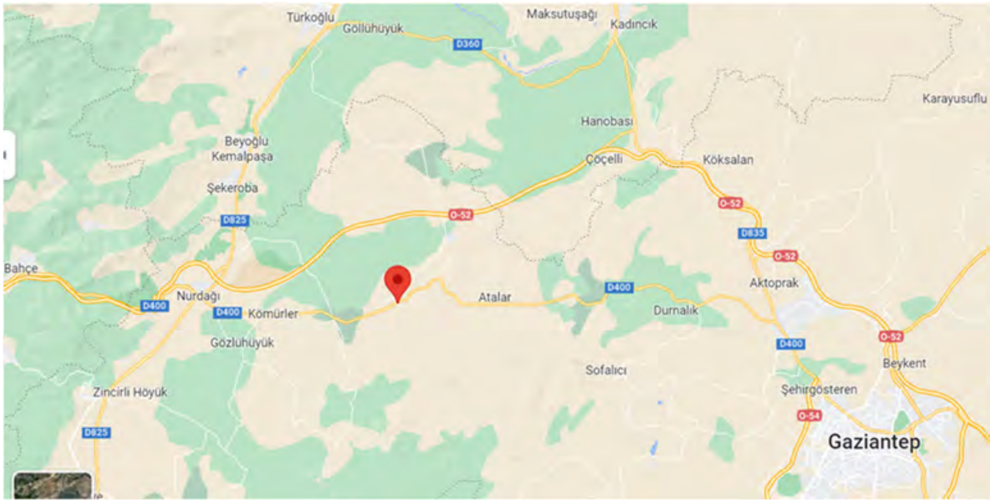

(Made using Google Maps)

Figure 2.5-3. Location of Sakcagoz between Gaziantep and Nurdağı

During the survey, traffic on the shoulder above the retaining wall was restricted using lane separator pole cones, as shown in **Figure 2.5-4**. A separation crack was observed between the pavement and the retaining wall, indicating that the retaining wall moved forward during the earthquake.

Figure 2.5-4. Traffic restriction on shoulder

Many buildings had also collapsed, as shown in **Figure 2.5-5**. A line earthwork was observed far from the town, but we had no time to visit and observe it.

Figure 2.5-5. Buildings in Sakcagoz

Figure 2.5-6 shows a cut slope example. No damage was observed.

Figure 2.5-6. Example of cut slopes